NANO LETTERS

Letter

pubs.acs.org/NanoLett

Tracking of Single Charge Carriers in a Conjugated Polymer Nanoparticle

Jiangbo Yu, Changfeng Wu,[†] Zhiyuan Tian,[‡] and Jason McNeill*

Department of Chemistry, Clemson University, South Carolina 29634, United States

Supporting Information

ABSTRACT: The motion of individual charge carriers in organic nanostructures was tracked by fluorescence microscopy. A twinkling effect is observed in fluorescence microscopy of single conjugated polymer nanoparticles, that is, small displacements in the fluorescence spot of single nanoparticles of the conjugated polymer PFBT are observed over time. There is evidence that superquenching by the charge carrier induces a dark spot in the nanoparticle, which moves with the carrier, resulting in the observed displacements in the fluorescence. Zero-field mobilities of individual charge carriers consistent with highly trapped polarons were obtained from tracking experiments.

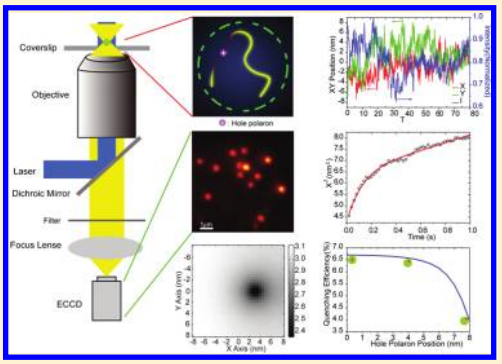

KEYWORDS: *Nanoscale tracking, conjugated polymer, carrier dynamics, hole polaron*

There is considerable interest in the use of semiconducting π-conjugated polymers and oligomers for a variety of applications, including light-emitting devices[1] and photovoltaic devices,[2] as well as emerging applications such as molecular electronics,[3−6] and fluorescent nanoparticles.[7−10] Conjugated polymers are molecular semiconductors in which conduction occurs through delocalized π-molecular orbitals. The presence of disorder as well as other effects typically results in hopping or dispersive charge transport,[11−13] which is in contrast to the free-electron-like motion of carriers in the highly delocalized band states of conventional crystalline semiconductors.

Conventional techniques for probing carrier transport, such as time-of-flight methods and current−voltage measurements,[14−18] involve averaging over large areas and large numbers of carriers. Optical imaging methods have been employed to monitor carrier dynamics in organic semiconductors,[19−21] but as yet these methods lack the ∼1 nm resolution and sensitivity required to directly image fundamental transport events of a single carrier. Application of single molecule spectroscopy to single conjugated polymer molecules and nanosized aggregates has revealed a number of unexpected and complex phenomena such as pronounced blinking due to quenching by hole polarons.[22−26] A combination of rapid intra- and interchain transport of excitons within the polymer and efficient energy transfer to nonfluorescent hole polarons causes hyperquenching; the loss of a single electron can quench up to 90% of the luminescence of a polymer chain consisting of hundreds or thousands of chromophore units.

The fundamental nature of charge transport and related phenomena in organic semiconductor materials is still a matter of considerable debate. Questions remain regarding the spatial extent of carrier or trap states, the distances and time scales of individual carrier "hopping" events, the detailed physical picture of the individual electron-transfer events, and how nanoscale structural heterogeneity and the resulting complex energy landscape dictate transport properties. In principle, such questions could be readily addressed by tracking the nanoscale motion of individual charge carriers in the semiconductor. In this Letter, we present a novel method for tracking the nanoscale motion of individual charge carriers in nanoparticles and demonstrate this method on nanoparticles of the conjugated polymer poly[(9,9-dioctylfluorenyl-2,7-diyl)-*co*-(1,4-benzo-{2,1′,3}-thiadiazole)] (PFBT). Employing fluorescence-based subnanometer-resolution tracking methods similar to those applied to the study of nanoscale protein dynamics and intracellular dynamics,[27−29] we observe fluctuations in the intensity and position of the particle fluorescence, somewhat similar to "twinkling" of stars. We propose that the fluctuations in position can be used to measure carrier motion, according to the following line of reasoning. Hole polarons effectively quench the luminescence of nearby chains, resulting in a dark spot in the nanoparticle. As polarons hop from site to site in the nanoparticle, the apparent position of the particle being imaged in a fluorescence microscope will be displaced due to changes in the position of the dark spot. These position fluctuations thus serve as a measure of nanometer-scale motion of hole polarons within the nanoparticle. Simulations of quenching by hole polarons in single nanoparticles indicate that the position fluctuations should be well above the measurement uncertainty. Applying video rate fluorescence microscopy to single

Received: October 26, 2011
Revised: January 26, 2012
Published: February 7, 2012

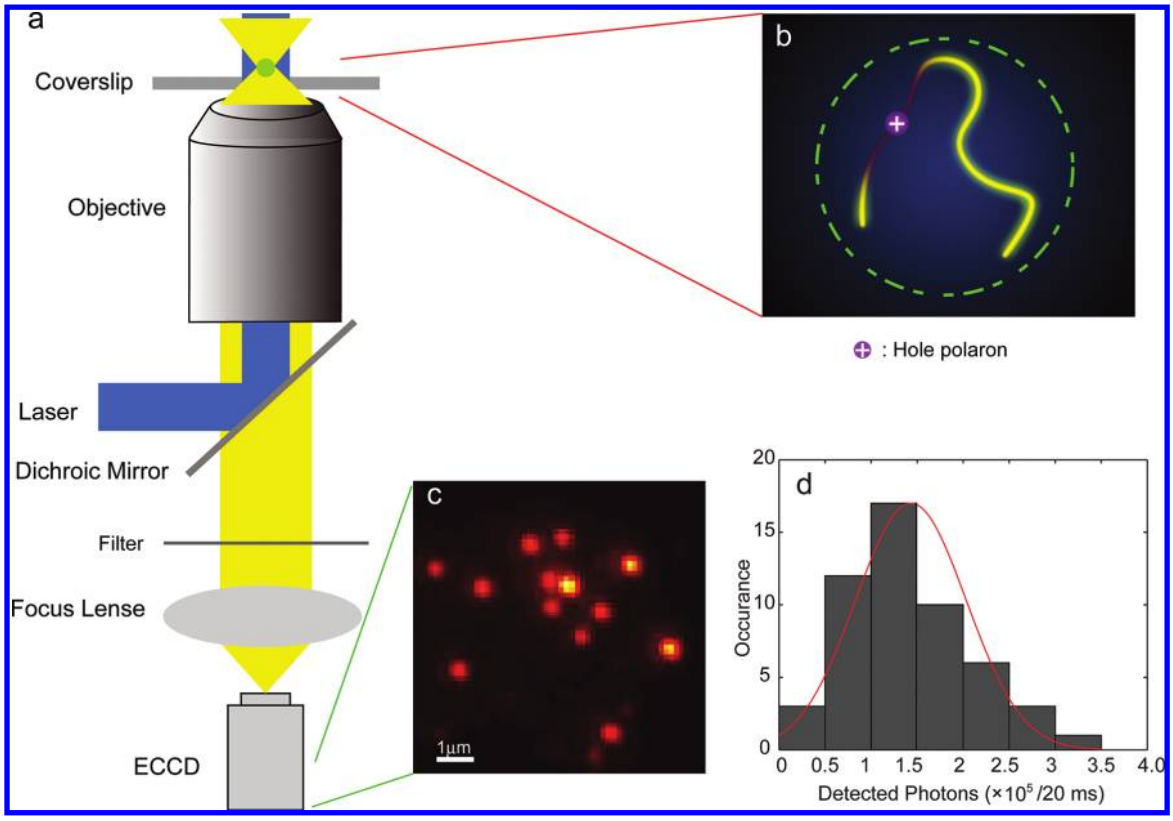

Figure 1. (a) Scheme showing the setup of the single particle tracking microscopy; (b) illustration representing the quenching of a single hole polaron on the exciton fluorescence, which is located at a single molecule chain within a single CPN; (c) a typical fluorescence CCD image of PFBT CPNs; (d) intensity histogram for CPNs at the excitation intensity of ~70 W/cm^2 (in the center of the laser spot), the red curve is obtained by fitting a 2D Gaussian to the histogram and gives 1.4 ± 0.6 × 10^5 (detected photons per 20 ms exposure).

conjugated polymer nanoparticles (CPNs), we have observed stepwise nanometer-scale fluctuations in the fluorescence intensity centroid, as well as smaller fluctuations. The mean square displacement of a centroid typically exhibits behavior consistent with confined diffusion, as expected for carriers trapped within a particle. Analysis of the results yields an average polaron diffusion constant of ~10^{-11} cm^2/s, corresponding to a zero field mobility of ~10^{-9} cm^2/V·s, markedly lower than that obtained for thin film devices, likely indicating the presence of deep traps associated with disorder or chemical defects in the conjugated polymer nanoparticles.

Nanoparticles of PFBT with diameters of 15 ± 4 nm were prepared and characterized as described previously (see Supporting Information, Figure S1a,b).[8] The particles were dispersed on a glass coverslip and imaged in an inverted fluorescence microscope (imaging setup illustrated in Figure 1a, with additional details provided in the Supporting Information). Under moderate laser excitation (473 nm, 70 W/cm^2), the bright yellow fluorescence of individual particles is readily observed with typically ~10^5 photons detected per particle per 20 ms exposure (Figure 1c,d.) On the basis of the width of the near-diffraction-limited spot and the fluorescence brightness, the 2D tracking uncertainty is typically ~0.7 nm (detailed determination provided in the Supporting Information). To determine the particle trajectories, areas of the sample were located that contained one or more larger particles or aggregates with steady fluorescence, which served as markers for correcting the trajectories for drift and vibration. A sequence of fluorescence microscopy images was acquired at a rate of 50 frames/second, for 160 s. The position trajectories were determined by least-squares fitting of a Gaussian function to the CCD image of fluorescence spot. The corrected position trajectories exhibit clear fluctuations well above the expected uncertainty based on the width of the fluorescence spot and signal levels (Figure 2a). Of the hundreds of particle trajectories analyzed, similar fluctuations were observed in the vast majority. The intensity trajectories also exhibit fluctuations above what is expected based on Poisson noise (Figure 2a), consistent with intensity fluctuations previously reported for single conjugated polymer molecules dispersed in an inert polymer matrix,[23,30,31] which were shown to be due to fluorescence superquenching by photogenerated hole polarons.[19,32−34]

In many cases, a 3D plot of *xy* centroid position versus time exhibits abrupt shifts in position, consistent with hopping or jumping behavior (representative single particle trajectory shown in Figure 2b). A comparison of position and intensity trajectories for the same particle (Figure 2c,d) indicates that at some points in the trajectory there are simultaneous jumps in fluorescence intensity and centroid positions, while at other points jumps in position occur with little change in fluorescence intensity and vice versa. These observations are consistent with photogeneration, recombination, and hopping behavior of polarons, discussed below. Additional trajectories, as well as their dependence on nanoparticle size, are provided in the Supporting Information.

Statistical analysis of several dozen trajectories was performed. The majority of particles exhibit a mean square displacement of the fluorescence along either axis, given by $\langle x_f^2(\tau)\rangle = \langle x_f^2(t+\tau) - x_f^2(t)\rangle$, which increases linearly for

dx.doi.org/10.1021/nl203784m | Nano Lett. 2012, 12, 1300−1306

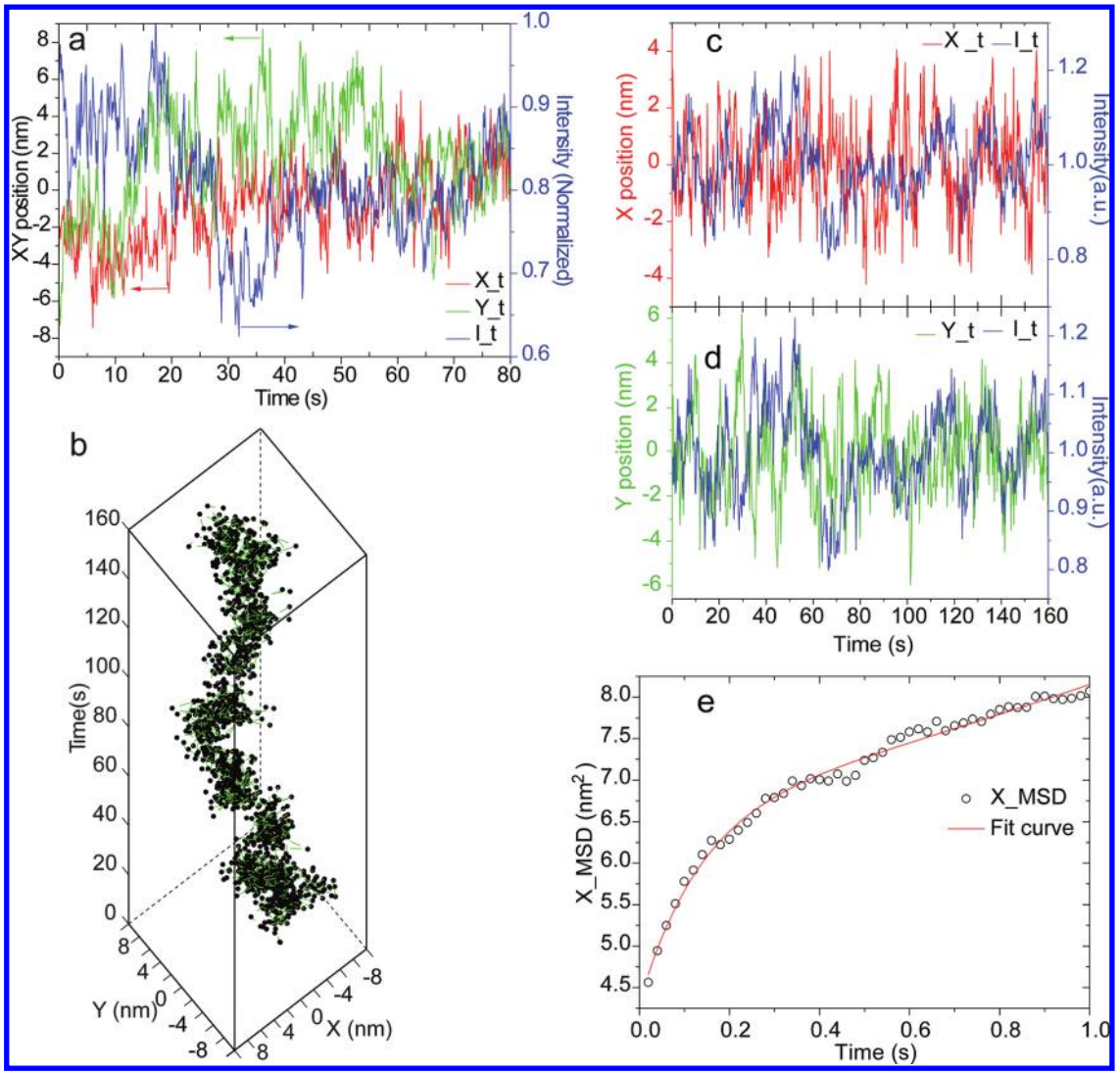

Figure 2. For the typical single nanoparticle. (a) The fluorescence intensity (normalized) and *xy* position trajectories: red (X), green (Y) and blue (I); (b) the 3D trajectory of the corrected *xy* position; (c) the trajectories of the corrected fluorescence intensity and centroid position, X and I trajectories; (d) Y and I trajectories; and (e) the mean square displacement along *x*-axis direction versus time $x_f^2(\tau)$ curve from 0 to 1.0 s, and its fit (red solid line) to the confined diffusion functional form, $\langle x_f^2(\tau)\rangle = \langle x_f^2(0)\rangle + L_f^2\{1 - \exp(-2D_f\tau/L_f^2)\}$ with fit parameters diffusion coefficient D_f and confined length L_f of 5.0 nm^2/s and 1.84 nm, respectively.

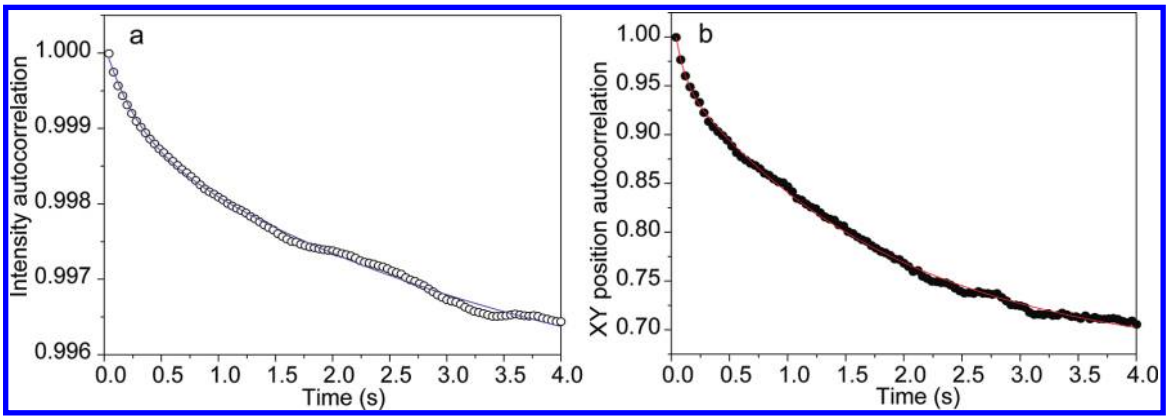

Figure 3. The intensity autocorrelation curve (a) with fit to the biexponential decay formula ($y = A_1e^{-x/\tau_1} + A_2e^{-x/\tau_2} + y_0$) to yield τ_1 = 0.28 s, τ_2 = 3.80 s, A_1 = 0.001, and A_2 = 0.004; and the *xy* position autocorrelation curve (b) of a single CPN with fit yielding τ_1 = 0.08 s, τ_2 = 1.87 s, A_1 = 0.072, and A_2 = 0.296.

roughly 0.2−0.4 s, then flattens as it approaches a plateau of 5−30 nm^2, as shown in Figure 2e, consistent with confined diffusion.[35−37] The phenomenological confinement length and diffusion constant of the position of the fluorescence spot were

dx.doi.org/10.1021/nl203784m | *Nano Lett.* 2012, 12, 1300−1306

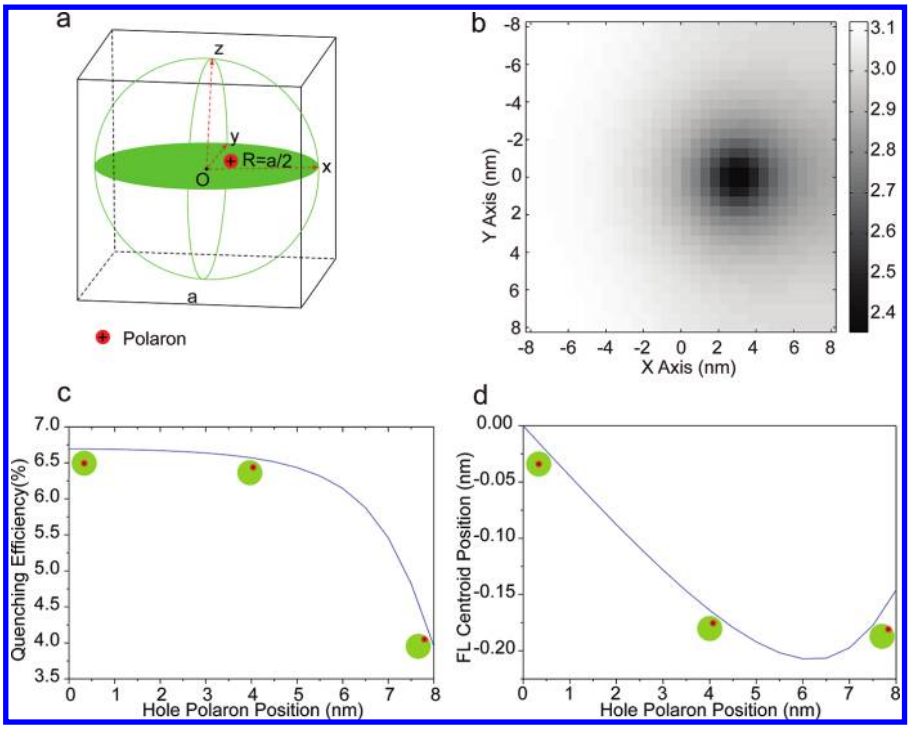

Figure 4. (a) A diagram showing a hypothetical single hole polaron within a CPN with 16 nm diameter. (b) Simulated near field fluorescence showing the exciton density projected on to the XY plane and the dark spot produced by the polaron quencher placed at 3 nm along *x*-axis, obtained from model of exciton diffusion and energy transfer. (c) Plot of quenching efficiency versus polaron position, obtained from model. (d) The simulated plot of fluorescence centroid position versus polaron position. Model results obtained with the FRET radius set to 2 nm and the exciton diffusion length set to 5 nm in a particle with 16 nm diameter. Details of the calculation are provided in the Supporting Information.

determined by fitting to a function of the form, $\langle x_f^2(\tau)\rangle = \langle x_f^2(0)\rangle + L_f^2\{1 - \exp(-2D_f\tau/L_f^2)\}$, yielding a typical value for the diffusion constant of the fluorescence centroid D_f of between 1.0×10^{-14} and 1.5×10^{-13} cm^2/s, and a typical value of the confinement length L_f ranging between 0.8 and 2.5 nm. The peaks in the distribution of values for D_f and L_f are 5×10^{-14} cm^2/s and 1.9 nm, respectively.

Autocorrelation of dozens of fluorescence centroid and intensity trajectories of CPNs were calculated (representative data shown in Figure 3a,b). Fitting the autocorrelations to a single exponential typically gave a poor fit (fitting results not shown), while fitting to a biexponential function (with an offset) yielded a significantly better fit, indicating heterogeneous dynamics. The time constants for the fit to the intensity autocorrelation results shown in Figure 3a are 0.28 and 3.80 s, while the fit to the position autocorrelation yielded time constants of 0.08 and 1.87 s (Figure 3b). The fit of the intensity autocorrelation included a relatively large offset (more than 99%), consistent with a low quenching efficiency of hole polarons reported previously.[38,39] When the time window of the data used in fitting was increased from 2 to 10 s, the time constants obtained from the fits also increased, consistent with heterogeneous dynamics spanning several time scales (see Figure S4 in the Supporting Information for fit results), and qualitatively consistent with models for charge transport in disordered media, which exhibit stretched-exponential[40,41] or power-law behavior.[42,43] Stretched-exponential and power law models also yielded good fits to the results (see Figure S5 in the Supporting Information).

Several possible explanations for the phenomena described above were considered, including motion of photogenerated charge carriers acting as fluorescence quenchers, quenching by long-lived triplet excitons, and photochemical degradation. It is highly unlikely that the fluctuations are due to quenching by triplet excitons, since the fluctuations observed in the present experiment are much too slow for triplet dynamics under the conditions employed.[44] While some photochemical degradation of the polymer occurs, the vast majority of intensity fluctuations observed are reversible, which rules out photochemical degradation as the principal cause of the fluctuations. Additionally, photochemical degradation occurs primarily on the >10 s time scale under the excitation conditions employed, significantly longer than the time scale of the position and intensity fluctuations. In contrast, several observations support charge carriers (specifically, hole polarons) as the principal cause of the observed intensity and centroid fluctuations. First, the time scale and amplitude of the fluctuations are consistent with several prior reports of intensity fluctuations associated with superquenching by hole polarons,[22,23] including electric field-modulation experiments,[20,32,34] which determined a quenching radius of 2−3 nm and unambiguously determined the charge of the quencher species. Fluctuations in polaron number are expected on the 0.5−10 s time scale under the excitation intensities employed (see Supporting Information). Additionally, the mean square displacement exhibited confined diffusion behavior at early lag times (<0.3 s), qualitatively consistent with the diffusion of charge carriers in a disordered material. Thus we conclude that the behavior of the mean square displacement at early lag times is primarily due to carrier (polaron) motion.

We developed a model to extract information about carrier motion from the fluctuations in the fluorescence centroid, described as follows. In the limiting case of a quencher with a small quenching efficiency and a quenching volume much

dx.doi.org/10.1021/nl203784m | *Nano Lett.* 2012, 12, 1300−1306

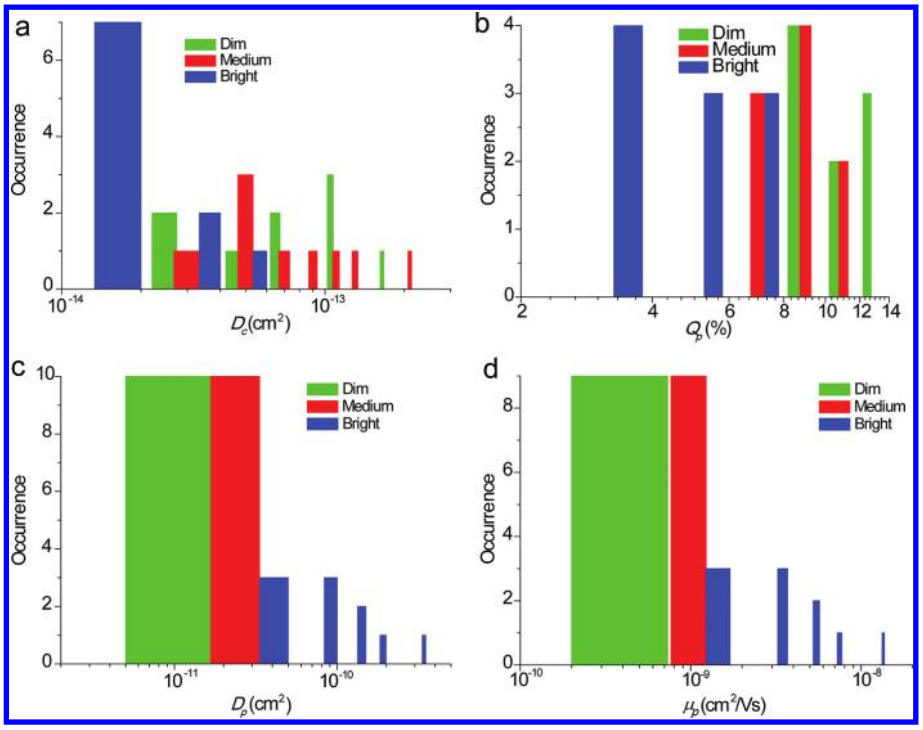

Figure 5. The histograms of the diffusion constants of the fluorescence centroids (a), the quenching efficiencies of the hole polarons (b), the diffusion constants of the hole polarons (c), and the mobilities of the hole polarons (d) for different single CPNs with different brightness (dim, medium, and bright).

smaller than the dimensions of a spherical or cube-shaped fluorescent particle, one obtains that the effect of the quencher on the fluorescence centroid is given by

$$\delta x_f = -x_q Q$$

where δx_f is the displacement of the fluorescence centroid due to the presence of the quencher, x_q is the position of the quencher relative to the center of the particle, and Q is the quenching efficiency of a single quencher. The quenching radius of a hole polaron in this polymer is likely in the range of 2−5 nm, so the conditions for the above expression are not met and therefore this expression is approximate. To test the approximate validity of this expression under the present conditions, calculations to determine the combined effects of exciton diffusion and energy transfer to hole polarons on the fluorescence centroid of a conjugated polymer nanoparticle were performed using an approach described previously (model parameters and calculation details provided in the Supporting Information).[45,46] The calculation results (Figure 4) indicate that the above expression is still accurate to within ∼35% for polarons located away from the particle surface. Thus, the above approximate expression can be used to roughly estimate changes in carrier position from changes in the fluorescence centroid.

The above expression relating quencher displacement to the fluctuations of the fluorescence centroid was used to estimate the charge carrier (hole polaron) mobility and confinement length as follows. The phenomenological diffusion constant of the fluorescence centroid (D_f) was obtained from the fit to the linear portion of the mean square displacement at short lag times (Figure 5a). Since the diffusion constant is related to the square of the displacement, and the factor relating displacement of the polaron to the displacement of the fluorescence centroid is the quenching efficiency Q_p, then the diffusion coefficient of the polaron is given by $D_p = D_f/Q_p^2$. The reported quenching efficiency for a single hole polaron depends on the polymer and the particle size, ranging from >50% for single PFBT molecules,[47] to less than 1% for a 30 nm nanoparticle of PFBT.[39] We estimated Q_p from the intensity trajectories of single nanoparticles (for details of the estimation method, see Supporting Information). For the nanoparticle trajectory shown in Figure 2, the Q_p is estimated from the intensity trajectory (shown in Figure S7 in Supporting Information) at 7.6%. Figure 5b shows a histogram of the quenching efficiency distribution for different single CPNs of various sizes (size estimated from the fluorescence brightness and size distribution as determined by AFM). We observed quenching efficiencies in the range of 3−13% with an average of around 8%. On the basis of these results, we calculated diffusion constants of hole polarons for dozens of nanoparticles (Figure 5c). The peak in the histogram corresponds to a polaron diffusion constant of $\sim 10^{-11}$ cm^2/s. Applying the Stokes−Einstein equation, estimated hole mobility values ranging from 10^{-10} $\sim 10^{-9}$ cm^2/V·s were obtained (Figure 5d). The calculation of the diffusion constant of the holes assumes a single hole polaron is present. On the basis of the individual stepwise intensity fluctuations and excitation intensities well below the saturation intensity,[45] we estimate that fewer than 10 polarons are typically present in a given particle. The effect of additional polarons on the mean square displacement analysis is discussed in the Supporting Information.

Reported zero-field mobility values obtained by current−voltage analysis of thin film devices containing derivatives of poly(phenylene vinylene) (PPV) or polyfluorene (PF) are typically in the range of 10^{-8}−10^{-7} cm^2/V·s,[48,49] while orders of magnitude higher mobility values are typically obtained by time-of-flight.[50−54] The broad range of reported mobility values can be attributed to differences in the techniques and in the

dx.doi.org/10.1021/nl203784m | Nano Lett. 2012, 12, 1300−1306

trap density, and level of disorder of the films. From the analysis of the fluctuations in the fluorescence centroid, we obtained a value for the zero field hole polaron mobility of roughly 10^{-9} $cm^2/V{\cdot}s$, which is 1−2 orders of magnitude lower than reported values obtained by *I*/*V*-analysis. It is likely that the nanoparticles would have additional conformational disorder, chemical defects, and energetic disorder, as compared to optimally prepared thin films. Additionally, in bulk thin film measurements the carrier density is typically high, hence a significant fraction of traps are filled,[14,55] while in the single CPN, the carrier density is likely lower, which would result in more trapping (more unfilled traps) and thus lower mobility. Another possible cause of the disagreement between thin film results and those reported here is the combined effect of the multiple time scales involved in carrier transport and the limited time resolution employed, which would lead to lower measured mobilities.

In conclusion, fluctuations in the fluorescence intensity and nanometer-scale displacements in the fluorescence centroid of single conjugated polymer nanoparticles were observed by video rate fluorescence microscopy. We attribute the fluctuations and displacements to the hopping motion of hole polarons, which effectively quench the fluorescence in the vicinity of the polaron, which is in agreement with prior reports and our simulations of energy transfer and exciton diffusion in nanoparticles. Simulations confirmed that the displacement in fluorescence centroid can act as a measure of polaron displacement. Analysis of the fluorescence displacement trajectories yielded hole polaron mobility values in a range consistent with highly trapped charge carriers, as expected based on the degree of disorder present in the particles. Furthermore, if we consider the observed polaron behavior in the nanoparticles to be somewhat representative of behavior within individual nanoscale regions in a bulk film, then the particle-to-particle variability in the determined polaron mobilities is consistent with some models or pictures of dispersive transport, in which nanoscale heterogeneity gives rise to large variability in the local transport properties. An alternative hypothesis is that the centroid fluctuations are primarily due to polaron generation and recombination events, however the generation and recombination rate is estimated to be significantly slower than the time scale of the observed fluctuations under the conditions employed. While the alternative hypothesis cannot be ruled out, on the basis of the preponderance of the evidence we conclude that displacements in the fluorescence centroid can be used to measure nanometer-scale motion and mobility of a single charge carrier within an organic semiconductor nanostructure.

■ ASSOCIATED CONTENT

Supporting Information

Details on the experimental methods, calculations, and additional data. This material is available free of charge via the Internet at http://pubs.acs.org.

■ AUTHOR INFORMATION

Corresponding Author

*E-mail: mcneill@clemson.edu.

Present Addresses

[†]State Key Laboratory on Integrated Optoelectronics, College of Electronic Science and Engineering, Jilin University, Changchun, 130012, People's Republic of China.

[‡]College of Chemistry and Chemical Engineering, Graduate University of the Chinese Academy of Sciences (GUCAS), Beijing, 100049, People's Republic of China.

Notes

The authors declare no competing financial interest.

■ ACKNOWLEDGMENTS

The authors gratefully acknowledge financial support from the NSF under Grant CHE-1058885 and from the NIH under Grant 1R01GM081040.

■ REFERENCES

(1) Friend, R. H.; Gymer, R. W.; Holmes, A. B.; Burroughes, J. H.; Marks, R. N.; Taliani, C.; Bradley, D. D. C.; Santos, D. A. D.; Bredas, J. L.; Logdlund, M.; Salaneck, W. R. Electroluminescence in conjugated polymers. *Nature* **1999**, *397* (6715), 121−128.

(2) Günes, S.; Neugebauer, H.; Sariciftci, N. S. Conjugated Polymer-Based Organic Solar Cells. *Chem. Rev.* **2007**, *107* (4), 1324−1338.

(3) Aviram, A.; Ratner, M. A. Molecular Rectifiers. *Chem. Phys. Lett.* **1974**, *29* (2), 277−283.

(4) Aviram, A. Molecules for Memory, Logic, and Amplification. *J. Am. Chem. Soc.* **1988**, *110* (17), 5687−5692.

(5) Kim, H. C.; Park, S. M.; Hinsberg, W. D. Block Copolymer Based Nanostructures: Materials, Processes, and Applications to Electronics. *Chem. Rev.* **2009**, *110* (1), 146−177.

(6) Zotti, G.; Vercelli, B.; Berlin, A. Monolayers and multilayers of conjugated polymers as nanosized electronic components. *Acc. Chem. Res.* **2008**, *41* (9), 1098−1109.

(7) Wu, C.; Bull, B.; Szymanski, C.; Christensen, K.; McNeill, J. Multicolor Conjugated Polymer Dots for Biological Fluorescence Imaging. *ACS Nano* **2008**, *2* (11), 2415−2423.

(8) Yu, J.; Wu, C.; Sahu, S. P.; Fernando, L. P.; Szymanski, C.; McNeill, J. Nanoscale 3D Tracking with Conjugated Polymer Nanoparticles. *J. Am. Chem. Soc.* **2009**, *131* (51), 18410−18414.

(9) Wu, C.; Schneider, T.; Zeigler, M.; Yu, J.; Schiro, P. G.; Burnham, D. R.; McNeill, J. D.; Chiu, D. T. Bioconjugation of Ultrabright Semiconducting Polymer Dots for Specific Cellular Targeting. *J. Am. Chem. Soc.* **2010**, *132* (43), 15410−15417.

(10) Pecher, J.; Mecking, S. Nanoparticles of Conjugated Polymers. *Chem. Rev.* **2010**, *110* (10), 6260−6279.

(11) Frenkel, J. On pre-breakdown phenomena in insulators and electronic semi-conductors. *Phys. Rev.* **1938**, *54* (8), 647−648.

(12) Hertel, D.; Bassler, H.; Scherf, U.; Horhold, H. H. Charge carrier transport in conjugated polymers. *J. Chem. Phys.* **1999**, *110* (18), 9214−9222.

(13) Arkhipov, V. I.; Emelianova, E. V.; Heremans, P.; Bassler, H. Analytic model of carrier mobility in doped disordered organic semiconductors. *Phys. Rev. B* **2005**, *72* (23), 235202/1−235202/5.

(14) Bässler, H. Injection, transport and recombination of charge carriers in organic light-emitting diodes. *Polym. Adv. Technol.* **1998**, *9* (7), 402−418.

(15) Fishchuk, I. I.; Arkhipov, V. I.; Kadashchuk, A.; Heremans, P.; auml; ssler, H. Analytic model of hopping mobility at large charge carrier concentrations in disordered organic semiconductors: Polarons versus bare charge carriers. *Phys. Rev. B* **2007**, *76* (4), 045210.

(16) Dunlap, D. H.; Parris, P. E.; Kenkre, V. M. Charge-Dipole Model for the Universal Field Dependence of Mobilities in Molecularly Doped Polymers. *Phys. Rev. Lett.* **1996**, *77* (3), 542−545.

(17) Tanase, C.; Meijer, E. J.; Blom, P. W. M.; de Leeuw, D. M. Unification of the Hole Transport in Polymeric Field-Effect Transistors and Light-Emitting Diodes. *Phys. Rev. Lett.* **2003**, *91* (21), 216601/1−216601/4.

(18) van Mensfoort, S. L. M.; Vulto, S. I. E.; Janssen, R. A. J.; Coehoorn, R. Hole transport in polyfluorene-based sandwich-type devices: Quantitative analysis of the role of energetic disorder. *Phys. Rev. B* **2008**, *78* (8), 085208/1−085208/10.

(19) McNeill, J. D.; Barbara, P. F. NSOM Investigation of Carrier Generation, Recombination, and Drift in a Conjugated Polymer. *J. Phys. Chem. B* **2002**, *106* (18), 4632−4639.
(20) McNeill, J. D.; Kim, D. Y.; Yu, Z. H.; O'Connor, D. B.; Barbara, P. F. Near-Field Spectroscopic Investigation of Fluorescence Quenching by Charge Carriers in Pentacene-Doped Tetracene. *J. Phys. Chem. B* **2004**, *108* (31), 11368−11374.
(21) Manaka, T.; Lim, E.; Tamura, R.; Iwamoto, M. Direct imaging of carrier motion in organic transistors by optical secondharmonic generation. *Nat. Photonics* **2007**, *1* (10), 581−584.
(22) Vanden Bout, D. A.; Kerimo, J.; Higgins, D. A.; Barbara, P. F. Near-Field Optical Studies of Thin-Film Mesostructured Organic Materials. *Acc. Chem. Res.* **1997**, *30* (5), 204−212.
(23) VandenBout, D. A.; Yip, W. T.; Hu, D. H.; Fu, D. K.; Swager, T. M.; Barbara, P. F. Discrete intensity jumps and intramolecular electronic energy transfer in the spectroscopy of single conjugated polymer molecules. *Science* **1997**, *277* (5329), 1074−1077.
(24) Hu, D. H.; Yu, J.; Barbara, P. F. Single-Molecule Spectroscopy of the Conjugated Polymer MEH-PPV. *J. Am. Chem. Soc.* **1999**, *121* (29), 6936−6937.
(25) Scheblykin, I.; Zoriniants, G.; Hofkens, J.; De Feyter, S.; Van der Auweraer, M.; De Schryver, F. C. Photoluminescence Intensity Fluctuations and Electric-Field-Induced Photoluminescence Quenching in Individual Nanoclusters of Poly(phenylenevinylene). *ChemPhysChem* **2003**, *4* (3), 260−267.
(26) Lin, H.; Tabaei, S. R.; Thomsson, D.; Mirzov, O.; Larsson, P.-O.; Scheblykin, I. G. Fluorescence Blinking, Exciton Dynamics, and Energy Transfer Domains in Single Conjugated Polymer Chains. *J. Am. Chem. Soc.* **2008**, *130* (22), 7042−7051.
(27) Dahan, M.; Levi, S.; Luccardini, C.; Rostaing, P.; Riveau, B.; Triller, A. Diffusion dynamics of glycine receptors revealed by single-quantum dot tracking. *Science* **2003**, *302* (5644), 442−445.
(28) Yildiz, A.; Forkey, J. N.; McKinney, S. A.; Ha, T.; Goldman, Y. E.; Selvin, P. R. Myosin V Walks Hand-Over-Hand: Single Fluorophore Imaging with 1.5 nm Localization. *Science* **2003**, *300*, 2061−2065.
(29) Huang, B.; Wang, W. Q.; Bates, M.; Zhuang, X. W. Three-dimensional super-resolution imaging by stochastic optical reconstruction microscopy. *Science* **2008**, *319* (5864), 810−813.
(30) Yu, J.; Hu, D.; Barbara, P. F. Unmasking Electronic Energy Transfer of Conjugated Polymers by Suppression of O2 Quenching. *Science* **2000**, *289* (5483), 1327−1330.
(31) Yu, J.; Song, N. W.; McNeill, J. D.; Barbara, P. F. Efficient Exciton Quenching by Hole Polarons in the Conjugated Polymer MEH-PPV. *Isr. J. Chem.* **2004**, *44*, 127−132.
(32) McNeill, J. D.; O'Connor, D. B.; Adams, D. M.; Barbara, P. F.; Kammer, S. B. Field-Induced Photoluminescence Modulation of MEH-PPV under near-Field Optical Excitation. *J. Phys. Chem. B* **2001**, *105* (1), 76−82.
(33) Barbara, P. F.; Gesquiere, A. J.; Park, S.-J.; Lee, Y. J. Single-Molecule Spectroscopy of Conjugated Polymers. *Acc. Chem. Res.* **2005**, *38* (7), 602−610.
(34) Gesquiere, A. J.; Park, S.-J.; Barbara, P. F. Hole-Induced Quenching of Triplet and Singlet Excitons in Conjugated Polymers. *J. Am. Chem. Soc.* **2005**, *127* (26), 9556−9560.
(35) Kusumi, A.; Sako, Y.; Yamamoto, M. Confined lateral diffusion of membrane receptors as studied by single particle tracking (nanovid microscopy). Effects of calcium-induced differentiation in cultured epithelial cells. *Biophys. J.* **1993**, *65* (5), 2021−2040.
(36) Wieser, S.; Moertelmaier, M.; Fuertbauer, E.; Stockinger, H.; Schütz, G. J. Un)Confined Diffusion of CD59 in the Plasma Membrane Determined by High-Resolution Single Molecule Microscopy. *Biophys. J.* **2007**, *92* (10), 3719−3728.
(37) Burada, P. S.; Hänggi, P.; Marchesoni, F.; Schmid, G.; Talkner, P. Diffusion in Confined Geometries. *ChemPhysChem* **2009**, *10* (1), 45−54.
(38) Palacios, R. E.; Fan, F.-R. F.; Bard, A. J.; Barbara, P. F. Single-Molecule Spectroelectrochemistry (SMS-EC). *J. Am. Chem. Soc.* **2006**, *128* (28), 9028−9029.
(39) Palacios, R. E.; Fan, F. R. F.; Grey, J. K.; Suk, J.; Bard, A. J.; Barbara, P. F. Charging and discharging of single conjugated-polymer nanoparticles. *Nat. Mater.* **2007**, *6* (9), 680−685.
(40) Im, C.; Lupton, J. M.; Schouwink, P.; Heun, S.; Becker, H.; Bassler, H. Fluorescence dynamics of phenyl-substituted polyphenylenevinylene-trinitrofluorenone blend systems. *J. Chem. Phys.* **2002**, *117* (3), 1395−1402.
(41) Felorzabihi, N.; Froimowicz, P.; Haley, J. C.; Bardajee, G. R.; Li, B. X.; Bovero, E.; van Veggel, F.; Winnik, M. A. Determination of the Forster Distance in Polymer Films by Fluorescence Decay for Donor Dyes with a Nonexponential Decay Profile. *J. Phys. Chem. B* **2009**, *113* (8), 2262−2272.
(42) Bagnich, S. A.; Konash, A. V. Kinetics of triplet-triplet annihilation in disordered organic solids on short time scale. *Chem. Phys.* **2001**, *263* (1), 101−110.
(43) Chaudhury, S.; Kou, S. C.; Cherayil, B. J. Model of Fluorescence Intermittency in Single Enzymes. *J. Phys. Chem. B* **2007**, *111* (9), 2377−2384.
(44) Yu, J.; Lammi, R.; Gesquiere, A. J.; Barbara, P. F. Singlet−Triplet and Triplet−Triplet Interactions in Conjugated Polymer Single Molecules. *J. Phys. Chem. B* **2005**, *109* (20), 10025−10034.
(45) Wu, C. F.; Zheng, Y. L.; Szymanski, C.; McNeill, J. Energy Transfer in a Nanoscale Multichromophoric System: Fluorescent Dye-Doped Conjugated Polymer Nanoparticles. *J. Phys. Chem. C* **2008**, *112* (6), 1772−1781.
(46) Tian, Z. Y.; Yu, J. B.; Wu, C. F.; Szymanski, C.; McNeill, J. Amplified energy transfer in conjugated polymer nanoparticle tags and sensors. *Nanoscale* **2010**, *2* (10), 1999−2011.
(47) Lammi, R. K.; Barbara, P. F. Influence of chain length on exciton migration to low-energy sites in single fluorene copolymers. *Photochem. Photobiol. Sci.* **2005**, *4* (1), 95−99.
(48) Blom, P. W. M.; de Jong, M. J. M.; Vleggaar, J. J. M. Electron and hole transport in poly(p-phenylene vinylene) devices. *Appl. Phys. Lett.* **1996**, *68* (23), 3308−3310.
(49) Bozano, L.; Carter, S. A.; Scott, J. C.; Malliaras, G. G.; Brock, P. J. Temperature- and field-dependent electron and hole mobilities in polymer light-emitting diodes. *Appl. Phys. Lett.* **1999**, *74* (8), 1132−1134.
(50) Lebedev, E.; Dittrich, T.; PetrovaKoch, V.; Karg, S.; Brutting, W. Charge carrier mobility in poly(p-phenylenevinylene) studied by the time-of-flight technique. *Appl. Phys. Lett.* **1997**, *71* (18), 2686−2688.
(51) Meyer, H.; Haarer, D.; Naarmann, H.; ouml; rhold, H. H. Trap distribution for charge carriers in poly(paraphenylene vinylene) (PPV) and its substituted derivative DPOP-PPV. *Phys. Rev. B* **1995**, *52* (4), 2587−2598.
(52) Fong, H. H.; Papadimitratos, A.; Hwang, J.; Kahn, A.; Malliaras, G. G. Hole Injection in a Model Fluorene−Triarylamine Copolymer. *Adv. Funct. Mater.* **2009**, *19* (2), 304−310.
(53) Kreouzis, T.; Poplavskyy, D.; Tuladhar, S. M.; Campoy-Quiles, M.; Nelson, J.; Campbell, A. J.; Bradley, D. D. C. Temperature and field dependence of hole mobility in poly(9,9-dioctylfluorene). *Phys. Rev. B* **2006**, *73* (23), 235201/1−235201/15.
(54) Khan, R. U. A.; Poplavskyy, D.; Kreouzis, T.; Bradley, D. D. C. Hole mobility within arylamine-containing polyfluorene copolymers: A time-of-flight transient-photocurrent study. *Phys. Rev. B* **2007**, *75* (3), 035215/1−035215/14.
(55) Arkhipov, V. I.; Heremans, P.; Emelianova, E. V.; Adriaenssens, G. J.; Bassler, H. Weak-field carrier hopping in disordered organic semiconductors: the effects of deep traps and partly filled density-of-states distribution. *J. Phys.: Condens. Matter* **2002**, *14* (42), 9899−9911.